# Supplementary Materials

# Design and Synthesis of Fluorescent Carbon Dot Polymer and Deciphering its Electronic Structure

Abhishek Sau[1,¥], Kallol Bera[1,¥], Uttam Pal[1,¥], Arnab Maity[1], Pritiranjan Mondal[1], Samrat Basak[1], Alivia Mukherjee[1], Biswarup Satpati[2], Pintu Sen[3] and Samita Basu[1,*]

[1]Chemical Sciences Division, [2]Surface Physics and Material Science Division, Saha Institute of Nuclear Physics, Kolkata 700 064, India, [3]Physics Department, Variable Energy Cyclotron Centre, Kolkata-700064, India

| Contents | | Pages |
|---|---|---|
| Section 1: | Synthesis of Ru(III) doped carbon dots, **Ru:CDs**, **Ru:CD-DTTs** and **Ru:CDβMEs** | 3 |
| Section 2: | Transmission electron micrograph of **CDs** and **Ru:CDs** | 3 |
| Section 3: | TEM and Spectroscopic properties of **Ru:CDβMEs** | 5 |
| Section 4: | Fluorescence Lifetime Measurement | 5-7 |
| . Section 5: | Electrochemical experiments by cyclic voltammeter. | 8 |
| Section 6: | Modeling of the polymeric carbon quantum dots | 9-14 |
| Section 7: | Plausible electron transfer path way and energy level diagram obtained from DFT calculations. | 15-17 |

## Section1: Synthesis of Ru(III) doped carbon dots, Ru:CDs and Ru:CD-DTTs.

**Materials and methods:** All the chemicals and solvents required for syntheses of **Ru:CD**, **Ru:CD-DTTs, Ru:CDβME** are of analytical grade. Citric acid (CA) ( ≥99.5%), ruthenium(III) chloride hydrate, dithiothritol (DTT) are purchased from Sigma Aldrich. Triple distilled water is used for the preparation of all the aqueous solutions. Solvents required for syntheses and spectroscopic studies have been purchased from SRL. Steady-state absorption and fluorescence spectra are recorded by using JASCO V-650 absorption spectrophotometer and Spex Fluoromax-3 Spectro-fluorimeter. Time-resolved emission spectra are traced using a picosecond pulsed diode laser based TCSPC fluorescence spectrometer and MCP-PMT as a detector. Respective transient intermediates are produced with third harmonic (355 nm) output of nanosecond flash photolysis set-up (Applied Photophysics) containing Nd:YAG (Lab series, Model Lab 150, Spectra Physics)[1]. TEM imaging is carried out using an FEI, TECNAI G2 F30, S-TWIN microscope operating at 300 kV equipped with a GATAN Orius SC1000B CCD camera. High-angle annular dark-field scanning/transmission electron microscopy (STEM-HAADF) is employed here using the same microscope. Cyclic voltammetry (CV) measurement is recorded with AUTOLAB-30 potentiostat/galvanostat. A platinum electrode and a saturated Ag/AgCl electrode are used as counter and the reference electrodes respectively. The glass carbon electrode is used as the working electrode. The cyclic voltammograms are recorded between -1 and 1V w.r.t. reference electrode at a different scan rate (2–20mV/s).

### a. Synthesis of Ru:CDs

**Ru:CDs** were synthesized in accordance with our previous report[1]. 1.0 gm of citric acid (CA) and 0.005 gm of $RuCl_3$ were dissolved in a 25 ml beaker, with 10 ml of Milli-Q water and then pyrolyzed using a hot plate with a magnetic stirrer at 150°C and 400 rpm for 5 hours. After 5 hours the solution was converted into yellow colored material which ensures the formation of **Ru:CDs.** It was then lyophilized and stored at 4°C.

### b. Synthesis of Ru:CD-DTTs:

A mixture of 500 mg of lyophilized **Ru:CDs** and 100 mg of 1, 4-Dithiothreitol (DTT) was refluxed in 3 ml of dimethyl formamide (DMF) at 120°C in stirring condition for 24 hours. After removal of DMF, excess DTT was removed by multiple washing with dichloromethane (DCM). A pure solution of **Ru:CD-DTTs** was collected and then lyophilized and stored at 4°C .

### c. Synthesis of Ru:CDβMEs:

A mixture of 500 mg of lyophilized **Ru:CDs** and 50 µl of β-Mercaptoethanol (βME) was refluxed in 3 ml of dimethyl formamide (DMF) at 120°C in stirring condition for 24 hours. After removal of DMF, excess βME was removed by multiple washing with DCM. A pure solution of **Ru:CDβMEs** was collected and then lyophilized and stored at 4°C.

## Section 2: Transmission electron micrograph

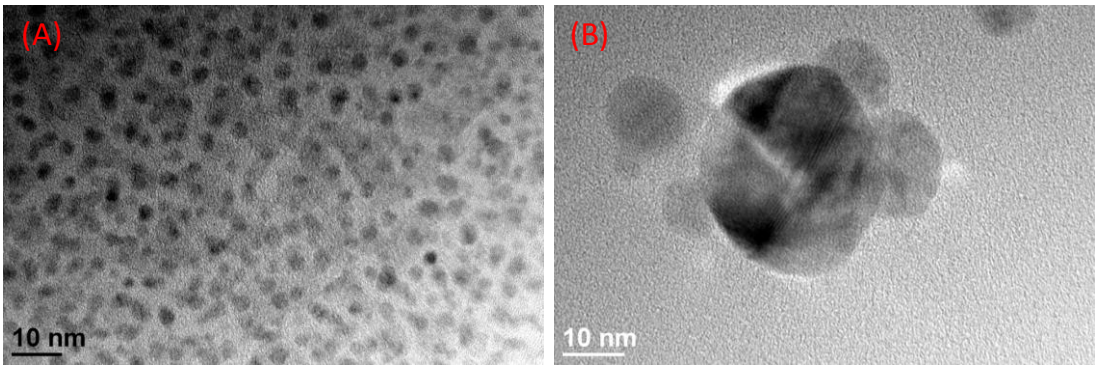


**Figure. S1.** Transmission electron micrograph of (A) only **CDs** (B) **Ru:CDs**

**Scheme S1: Synthetic root of Ru:CDβMEs.**

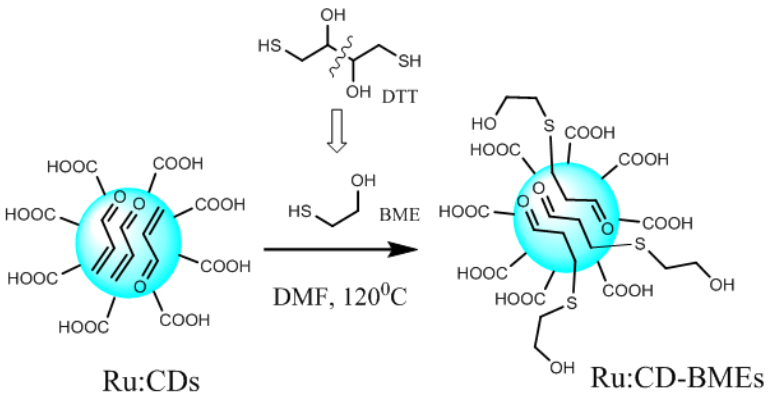

## Section 3: TEM and Spectroscopic properties of Ru:CDβMEs

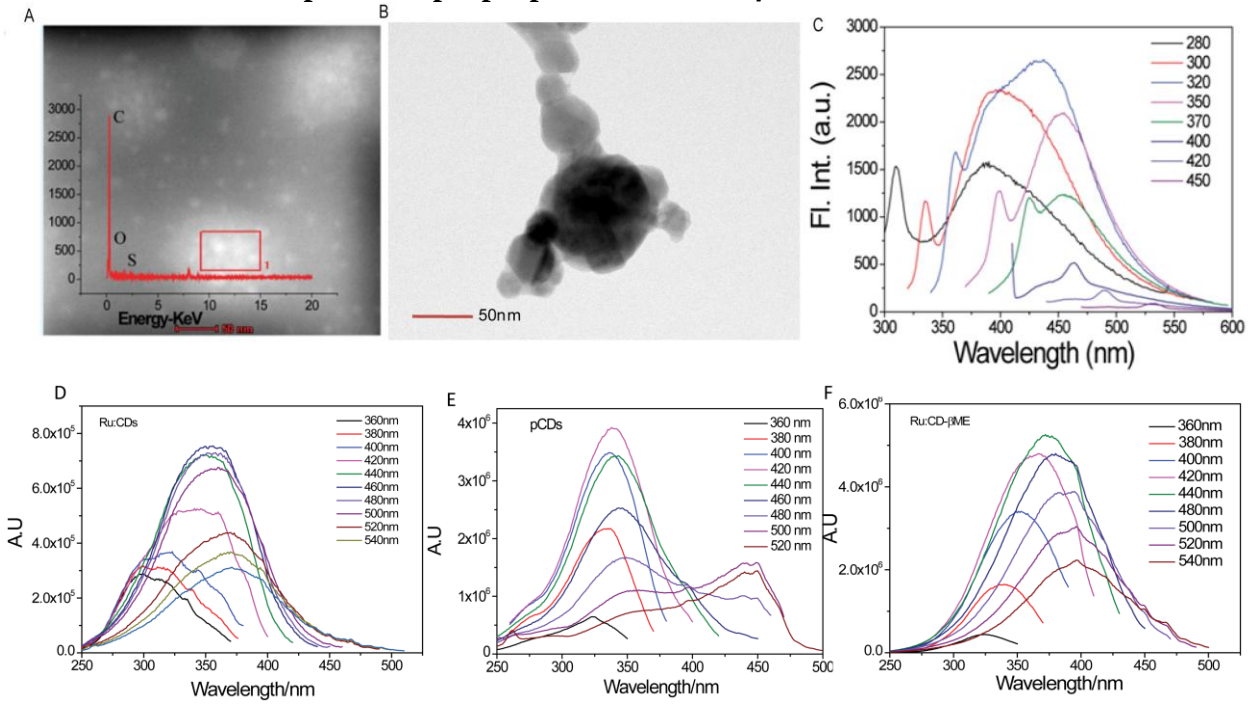


**Figure. S2:** (A) STEM-HADF image of **Ru:CDβMEs** area was chosen for EDX mapping (index: EDX map) (B) TEM image of aggregated **Ru:CDβMEs (C)** Photoluminescence of **Ru:CDβMEs** obtained at different excitation wavelengths, progressively increasing from 300 nm to 450 nm; Excitation spectra of (D) **Ru:CDs** (E) **Ru:CD-DTTs** (F) **Ru:CDβMEs.**

## Section 4: Fluorescence Lifetime Measurement.

The fluorescence lifetime measurement was performed using a picosecond pulsed diode laser based TCSPC fluorescence kinetic spectrometer with $\lambda_{ex}$= 280, 295, 340, 375 nm and MCP-PMT as a detector. The emission from the samples were collected at a right angle to the direction of the excitation beam maintaining magic angle polarization (54.7•) with a band pass of 2 nm. The full width at half maximum (FWHM) of the instrument response function was 270 ps and the resolution was 28 ps per channel. The data were fitted to exponential functions after deconvolution of the instrument response function by an iterative reconvolution technique using data analysis software, in which reduced $\boldsymbol{\varkappa^2}$ and weighted residuals serve as parameters for better fit. All the steady-state and time-resolved measurements were performed at room temperature (298 K).

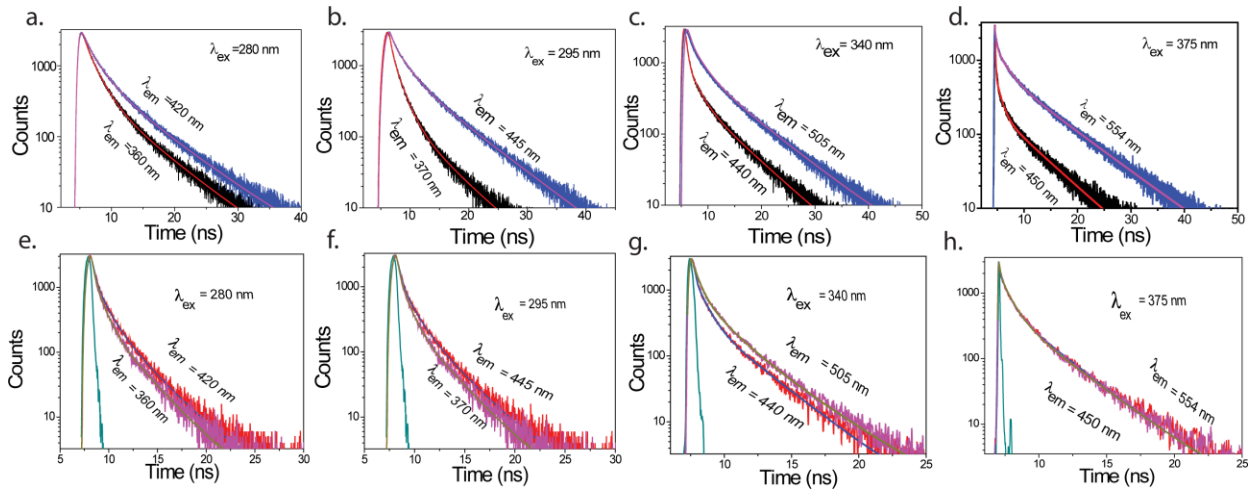


**Figure. S3:** Fluorescence decay profiles of (a→ d) **Ru:CD-βMEs ;** (e→ h) **Ru:CDs** at different excitation wavelengths. [$\lambda_{ex}$ = 280, 295, 340 and 375 nm]

**Table S1:** Fluorescence life times (τ) with corresponding % contributions (α) of (a) **Ru:CDs** (b) **Ru:CD-βMEs** at different excitation wavelengths ($\lambda_{ex}$).

| (A) $\lambda_{excitation}$ (nm) | $\lambda_{emission}$ (nm) | $\tau_1$ ns | $\alpha_1$ | $\tau_2$ ns | $\alpha_2$ | $\tau_3$ ns | $\alpha_3$ | <τ> ns |
|---|---|---|---|---|---|---|---|---|
| 280 | 360 | 4.3 | 24.82 | 1.8 | 55.38 | 9.31 | 19.80 | 6.02 |
| | 420 | 1.8 | 65.2 | 5.9 | 29. 46 | 15.5 | 5. 35 | 6.7 |
| 295 | 370 | 1.7 | 40.43 | 8.3 | 34.16 | 5.38 | 25.41 | 6.5 |
| | 445 | 2.13 | 36.52 | 8.57 | 31.04 | 5.66 | 32.45 | 6.6 |
| 340 | 440 | 1.4 | 33.44 | 7.3 | 35.04 | 1.2 | 31.32 | 5.8 |
| | 505 | 3.2 | 33.72 | 0.95 | 36.29 | 8.5 | 29.99 | 6.3 |
| 375 | 450 | 1.2 | 34.6 | 5.38 | 60.4 | 0.64 | 5 | 5.8 |
| | 554 | 1.5 | 39.39 | 6.56 | 52.43 | 0.16 | 8.18 | 5.7 |

| (B) $\lambda_{excitation}$ (nm) | $\lambda_{emission}$ (nm) | $\tau_1$ ns | $\alpha_1$ | $\tau_2$ ns | $\alpha_2$ | $\tau_3$ ns | $\alpha_3$ | <τ> ns |
|---|---|---|---|---|---|---|---|---|
| 280 | 360 | 1.79 | 54.40 | 0.40 | 9.60 | 6.08 | 36.01 | 4.70 |
| | 420 | 2.24 | 39.33 | 6.66 | 47.95 | 0.35 | 12.72 | 5.64 |
| 295 | 370 | 1.46 | 47.34 | 0.15 | 31.42 | 5.36 | 21.25 | 3.79 |
| | 445 | 2.29 | 34.45 | 6.99 | 54.25 | 0.36 | 11.30 | 6.12 |
| 340 | 440 | 1.72 | 21.04 | 6.31 | 39.05 | 0.04 | 39.91 | 5.69 |
| | 505 | 2.13 | 29.44 | 7.37 | 58.16 | 0.27 | 12.41 | 6.65 |
| 375 | 450 | 0.96 | 21.67 | 6.58 | 58.37 | 0.08 | 19.96 | 6.26 |
| | 554 | 1.96 | 21.29 | 8.12 | 72.53 | 0.28 | 6.18 | 7.69 |

**Table S2:** Fluorescence life times (τ) with corresponding % contributions (α) of **Ru:CD-DTTs** with the gradual addition of MQ (10 μM -100 μM) ($\lambda_{ex}$=340 nm).

| **Ru:CDDTT+MQ** | $\tau_1$ | $\alpha_1$ | $\tau_2$ | $\alpha_2$ | $\tau_3$ | $\alpha_3$ | <τ> |
|---|---|---|---|---|---|---|---|
| Ru:CD-DTT | 2.22 | 28.31 | 8.3 | 56.54 | 0.32 | 15.10 | 7.5 |
| Ru:CD-DTT+10μMMQ | 2.00 | 28.33 | 7.8 | 46.72 | 0.34 | 24.45 | 6.89 |
| Ru:CD-DTT+50μMMQ | 2.05 | 30.15 | 7.3 | 43.24 | 0.33 | 26.61 | 6.30 |
| Ru:CD-DTT+100μMMQ | 2.1 | 30.67 | 6.8 | 41.39 | 0.38 | 27.94 | 5.75 |

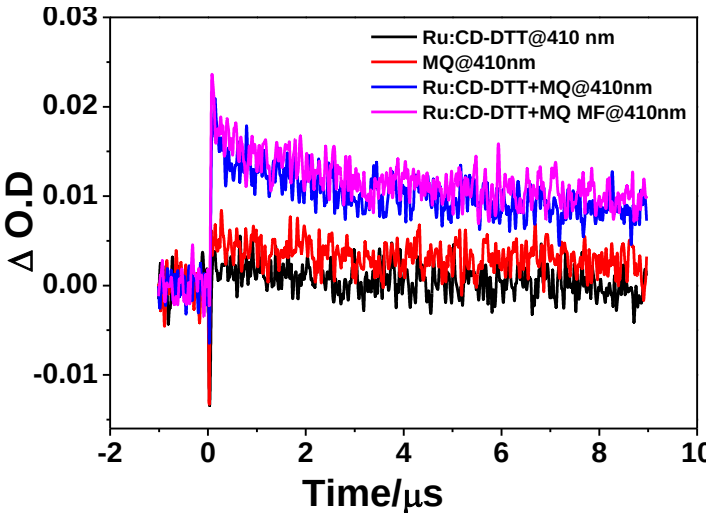


**Figure S4:** Decay profile of the transient at 410 nm in absence (blue line) and presence (purple line) of MF (0.08 T).

## Section 5: Electrochemical experiment by cyclic voltammeter.

A platinum electrode and a saturated Ag/AgCl electrode were used as counter and the reference electrodes respectively. The glass carbon electrode was used as the working electrode. The cyclic voltammograms were recorded between -1 and 1V. PBS buffer (10mM; pH=7.2±0.2) was used as the electrolyte. The concentration of the MQ is varied from 0.5mM→1.5mM by gradual addition to **Ru:CD-DTTs [**1mg/ ml] in PBS buffer.

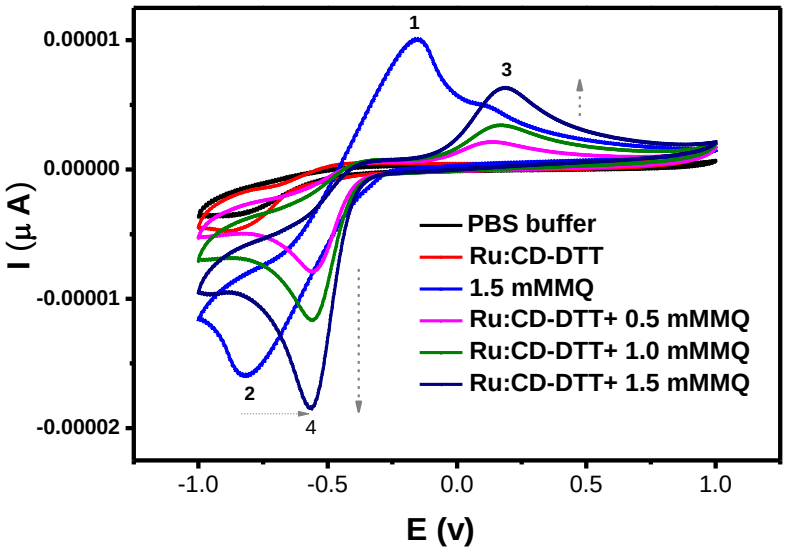


**Figure S5:** Cyclic voltammogram (6 scans average) for only **PBS** buffer, **Ru:CD-DTTs**, **MQ** (1.5 mM) and **Ru:CD-DTTs-MQ** (0.5→1.5mM) in PBS buffer (10mM; pH=7.2±0.2) with respect to SCE and glass carbon electrode as a working electrode..

## Section 6: Modeling of the polymeric carbon dot (CDs)

**Molecular mechanical studies.** Atomic models of citric acid pyrolysation products (Fig. S6), their DTT linked counterparts and dimerization products (Fig. S7) are drawn in Avogadro[2] and energy is minimized using steepest descent followed by conjugate gradient algorithms using universal force field (UFF) as implemented in Avogadro. Packmol[3] is used for packaging of these molecules into spherical **pCDs**. Two sets of **pCDs** are developed: one set with layer by layer addition of the molecules of increasing molecular weight (Fig. S9 ) and the other set without a layered structure (Fig. S8,S10). DTT modified **pCDs** are developed by placing the DTT linked molecules on the outer shell/surface with DDT pointing outward (Fig. S11a). For MQ coated **pCDs**, MQ is linked through the DDT (Fig. S11b). Polymerizations of **pCDs** are modeled by linking two or more **pCDs** via DTT (Fig. S11). PyMOL molecular graphics system is used to make the polymeric **pCDs**. The subsequent energy minimization of the **pCDs** and their polymers are done in Schrodinger Maestro molecular modeling environment. Molecular dynamics are performed using Desmond molecular dynamics program[4]. All the dynamic simulations are run under OPLS (optimized potentials for liquid simulations) force field[5]. OPLS forcefield provides a broad coverage to the drug-like small molecules apart from the biomacromolecules[5], which has made it a suitable choice for the **pCD** simulations. Before the simulations in water medium, **pCDs** are subjected to a relaxation step with unrestrained dynamics in vaccuo for 100 ps. The **pCDs** are placed at the center of a periodic boundary box with a minimum distance of 10 Å from each side. Number of atoms (N) and the volume of the system (V) are constant throughout the simulation and the system has a defined temperature (T) of 300 K. During this cooking in pressure cooker stage (NVT ensemble), intermolecular contacts are formed and the **pCDs** become more compact and geometry optimized for the production MD. These compact **pCDs** are then solvated using SPC (single point charge) water model and a NPT ensemble is defined with

a constant number of atoms (N), constant pressure (P) of 1 bar and a defined temperature of 300K. Nose-Hoover thermostat and Martyna-Tobias-Klein barostat are used in this simulation with relaxation time of 1 and 2 ps, respectively. The production MDs are run for 48 ns each for the different **pCDs** and their polymers. Simulation trajectory analysis to probe the deviations from initial conformation (RMSD), radius of gyration (Rg), hydrogen bonding with the solvents and intermolecular hydrogen bonding (Fig. S13) etc. is performed in Schrodinger Maestro and Visual Molecular Dynamics[6] software of University of Illinois.

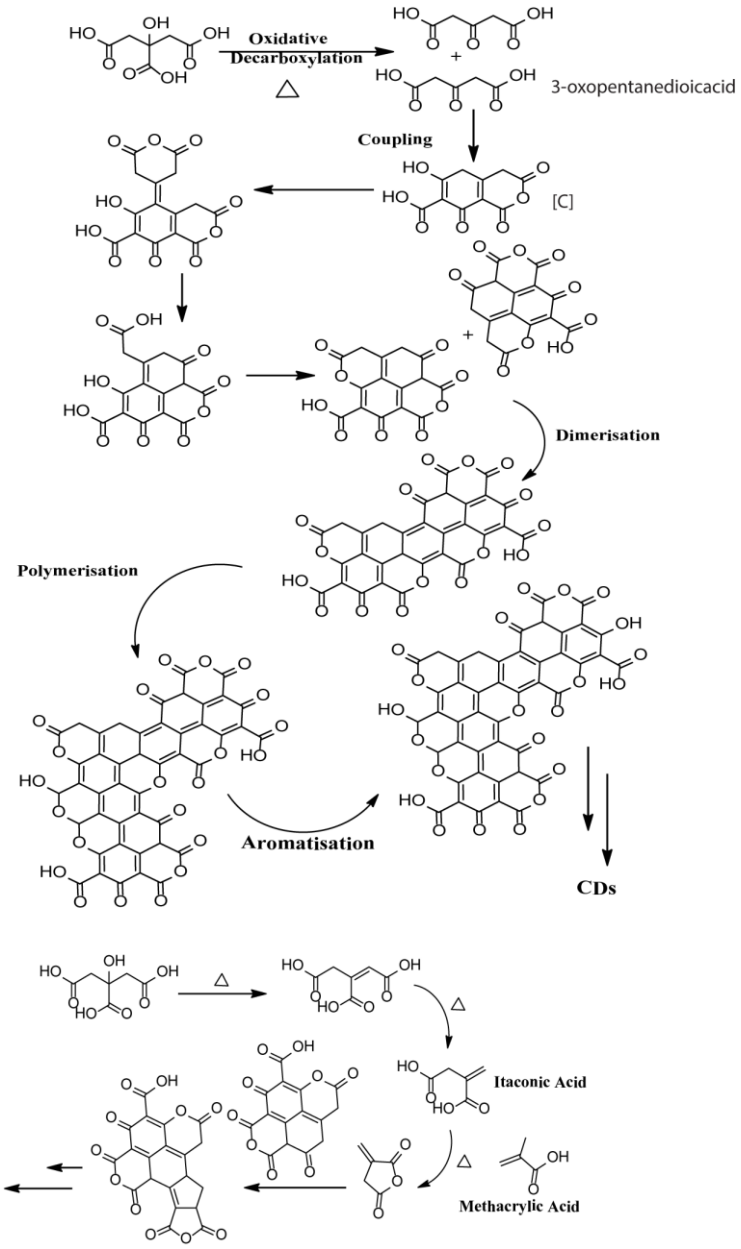

b.

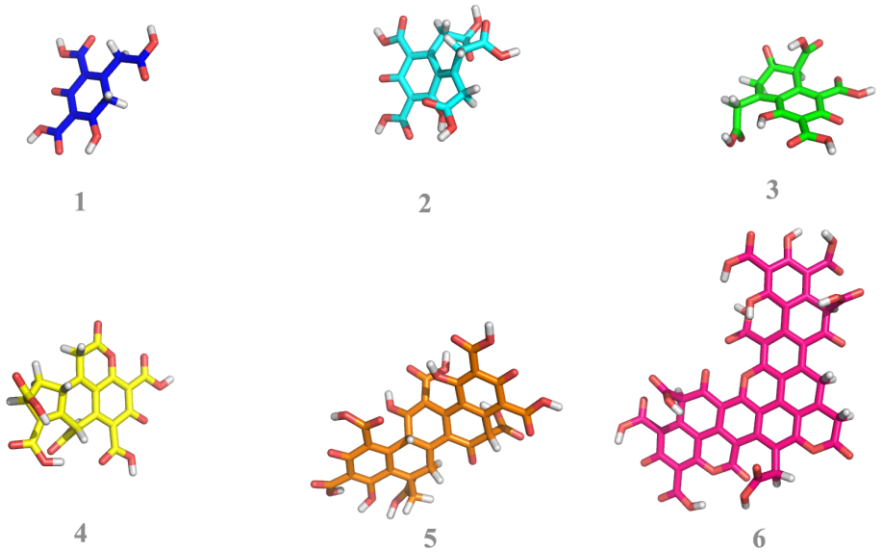


**Figure S6:** (a) Plausible mechanism for gradual formation of nanodomain of **CDs**[7]. (b) building blocks-1, 2, 3, 4, 5, 6. [blue ended to red ended moieties] formed by oxidative decarboxylation followed by acid catalyzed condensation reaction of citric acid.

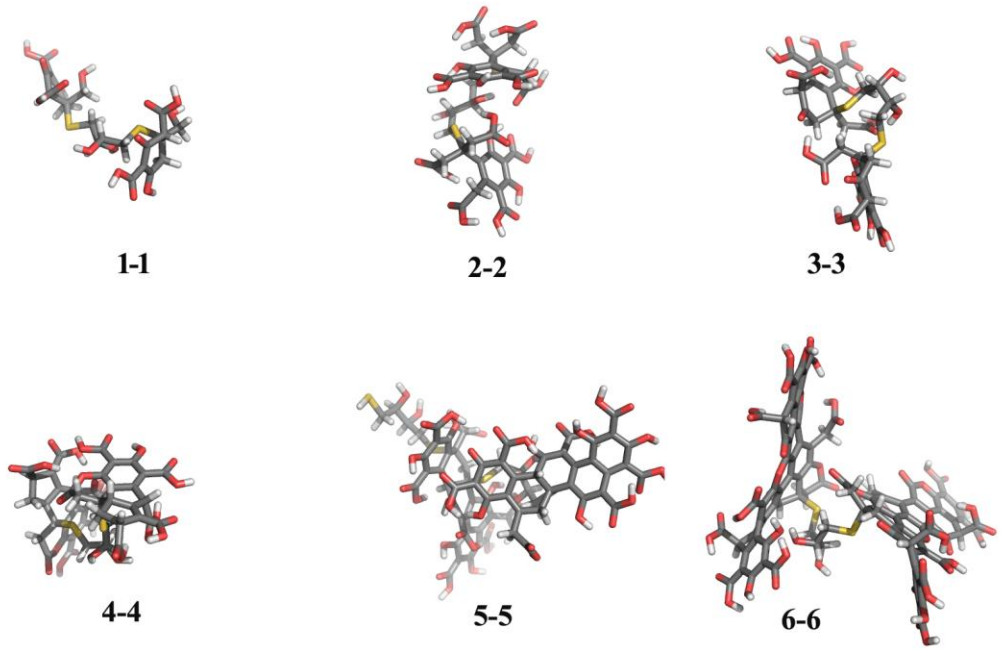


**Figure S7:** Crosslinking and formation of homodimers of building blocks-1, 2, 3, 4, 5, 6.

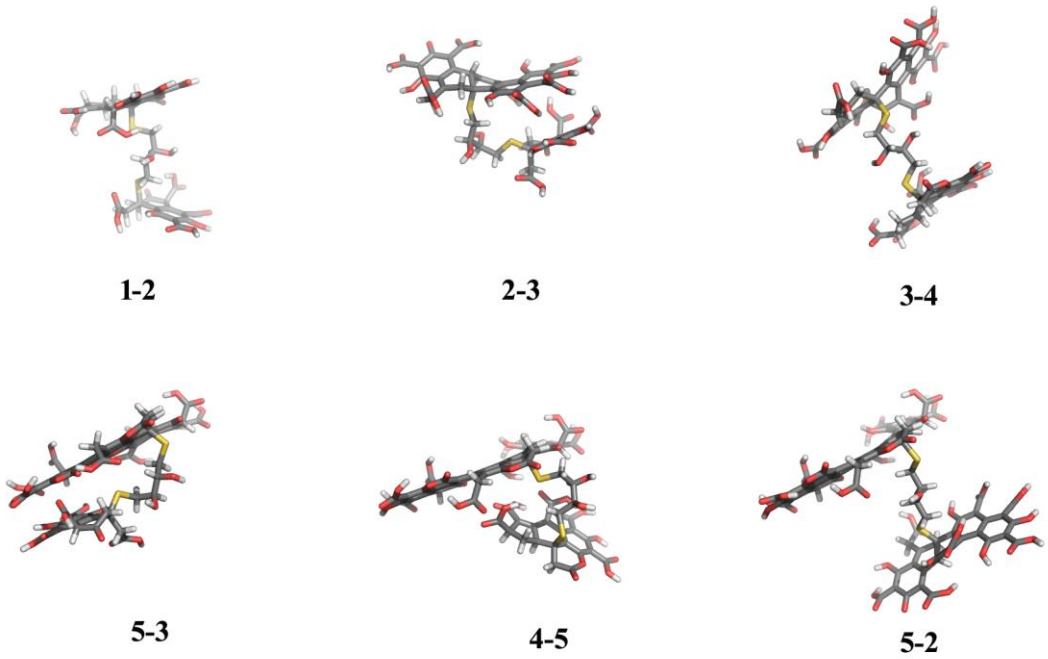


**Figure S8:** Crosslinking and formation of heterodimers of building blocks-1, 2, 3, 4, 5, 6.

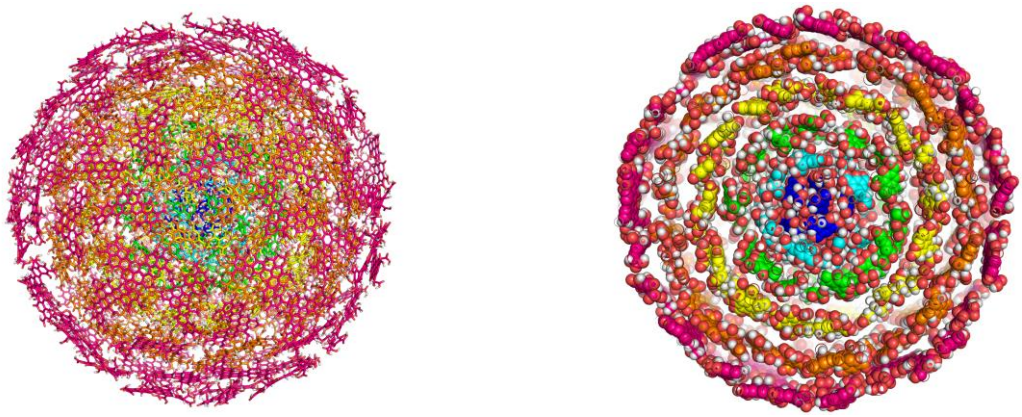

**Figure S9:** Formation of the (a) homogeneous nano structure along with its cross section.

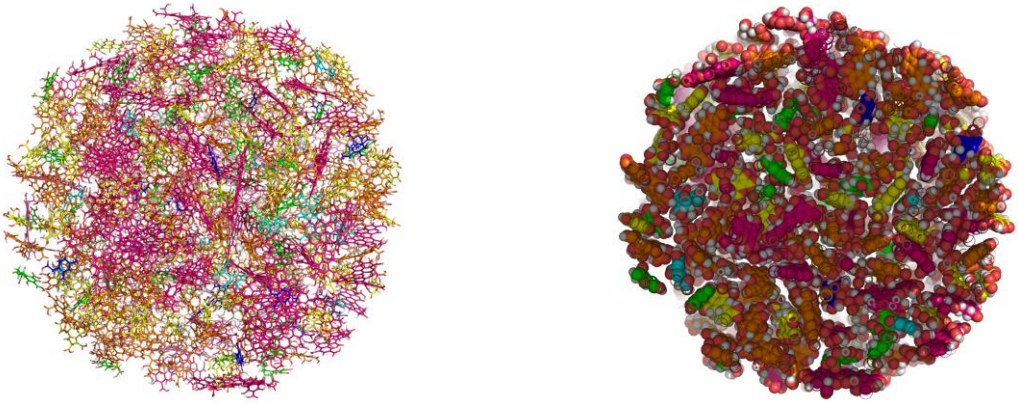

**Figure S10:** Formation of the (a) heterogeneous nano structure along with its cross section.

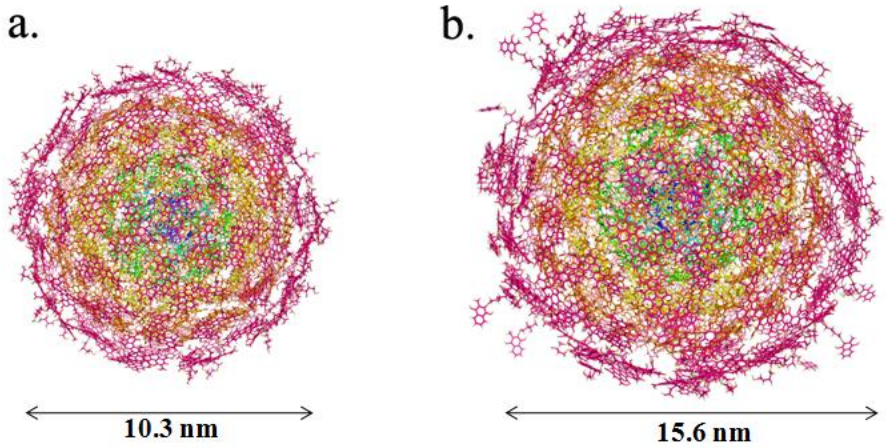


**Figure S11:** (a) **DTT** modified **CDs** (b) **MQ** linked **CD-DTTs.**

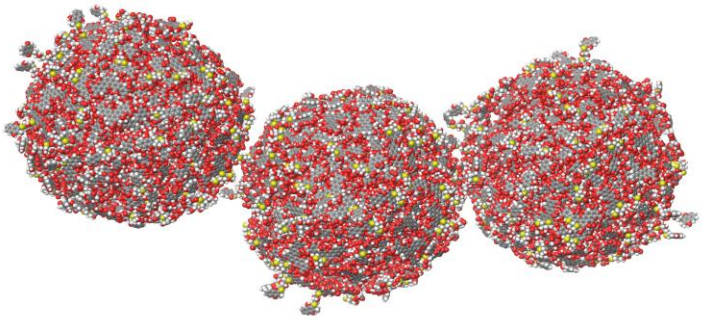

**Figure S12:** Menadione (MQ) attached **pCD-DTTs**.

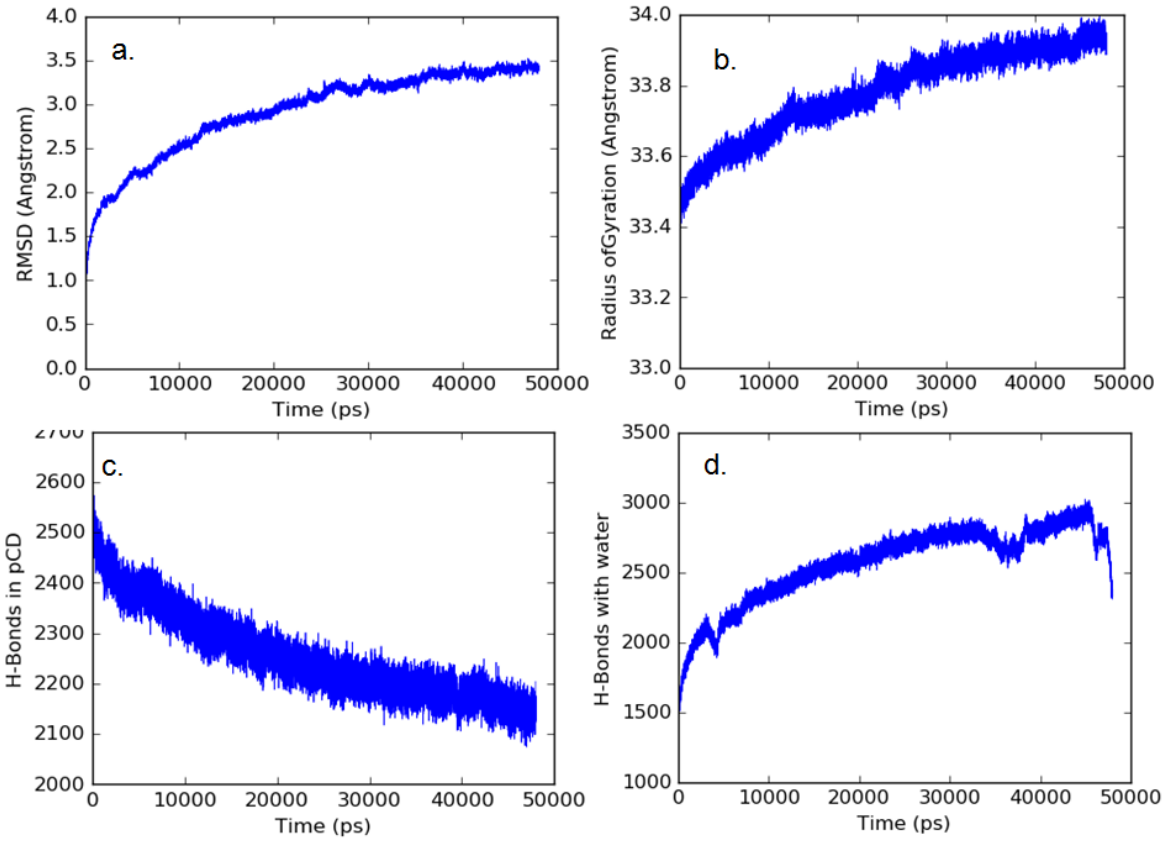


**Figure S13:** (a) Root mean square deviation (rms) of the **pCDs** with respect to time; (b) Radius of gyration with respect to time (c) Intermolecular hydrogen bonding among the building blocks of **pCDs**. (d) Hydrogen bonding with water.

## Section 7: Plausible electron transfer path way and energy level diagram obtained from DFT calculations.

**Quantum mechanical analysis:** Photo induced electron transfer (PET) processes are studied using the ab initio quantum mechanical methods. Geometries of the building blocks, their DTT linked forms, menadione (keto and enol) and menadione-stacked/linked-building-blocks are optimized using density functional theory (DFT) with B3LYP (Becke, 3-parameter, Lee-Yang-Parr) hybrid functional. Pople's split-valence double-zeta basis set with added s and p diffuse functions and d polarization functions on non-hydrogen atoms: 6-31g+(d) is used for the calculations. The calculations are performed in the presence of water by placing the solute molecules in a cavity within the solvent field. The Polarizable Continuum Model (PCM) using the integral equation formalism variant (IEFPCM) is used to describe the implicit solvent. In order to obtain frequency dependent response properties, excitation energies and their photo absorption spectra, time dependent (TD) DFT calculations are performed on these molecules using the same level of theory. All the ab initio calculations are done in the Gaussian 09 program (revision D.01). Molecular orbital energies of the building blocks are compared to that of free and bound menadione (both keto and ennol forms) and shown in (Fig. S14 A→F). All the possible electronic transitions for the building blocks are analyzed to find their donor/acceptor efficiency. Theoretical absorption spectra of the building blocks are also obtained from the TD-DFT calculations.

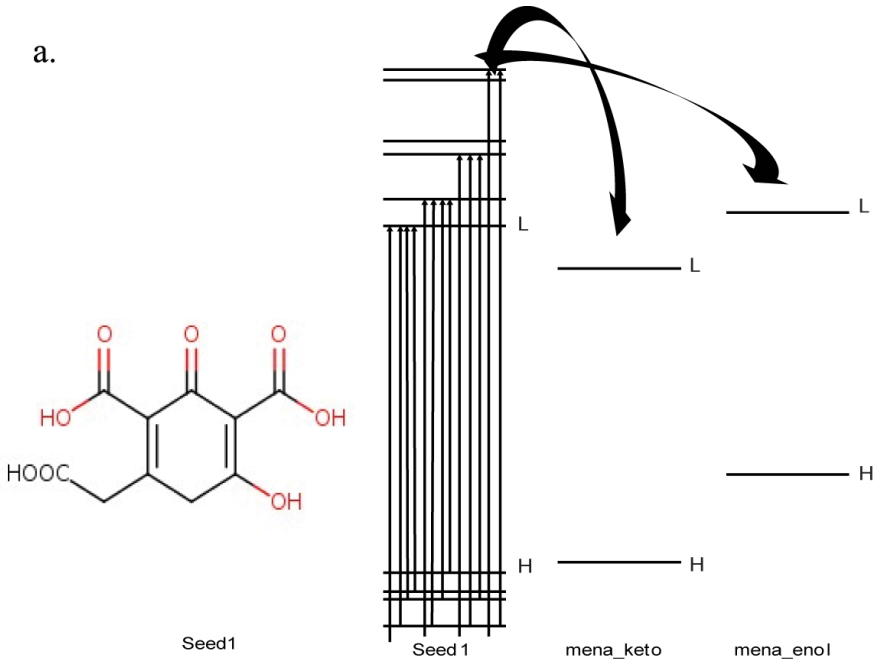

b.

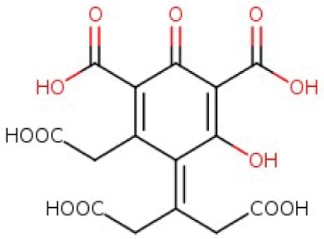


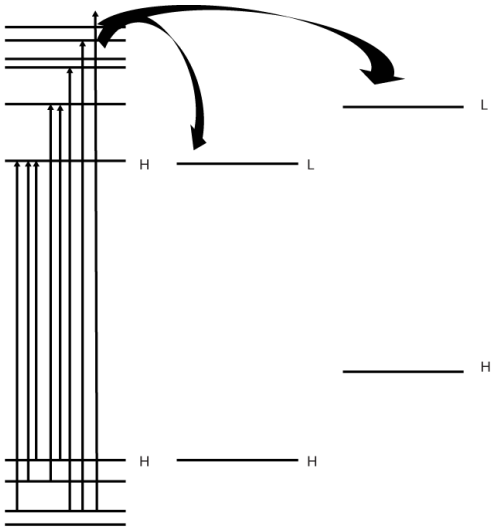


Seed 2 Seed 2 mena_keto mena_enol

c.

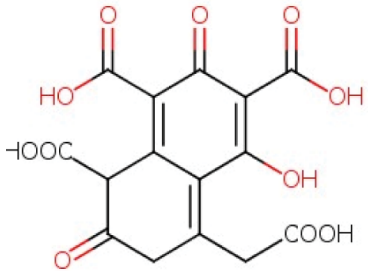


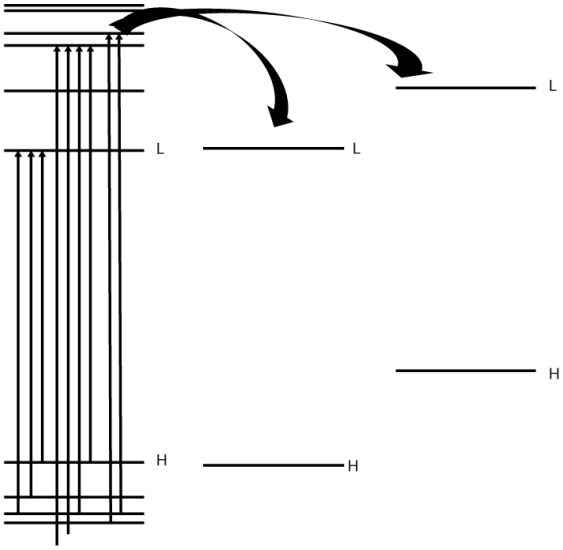


Seed 3 Seed 3 mena_keto mena_enol

d.

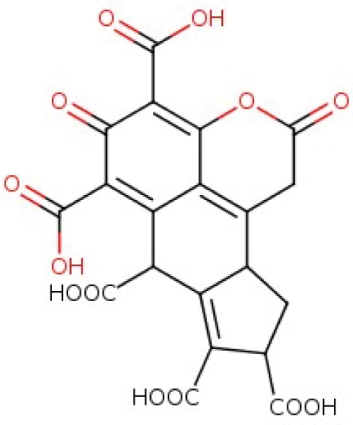


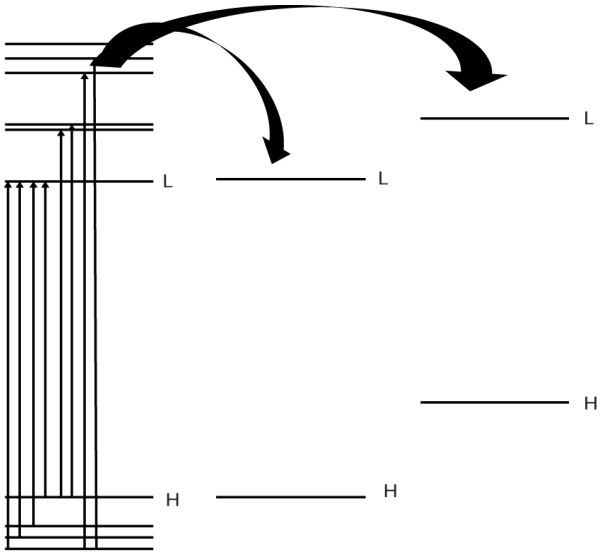


Seed 4 Seed 4 mena_keto mena_enol

e.

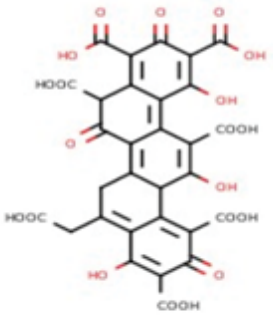


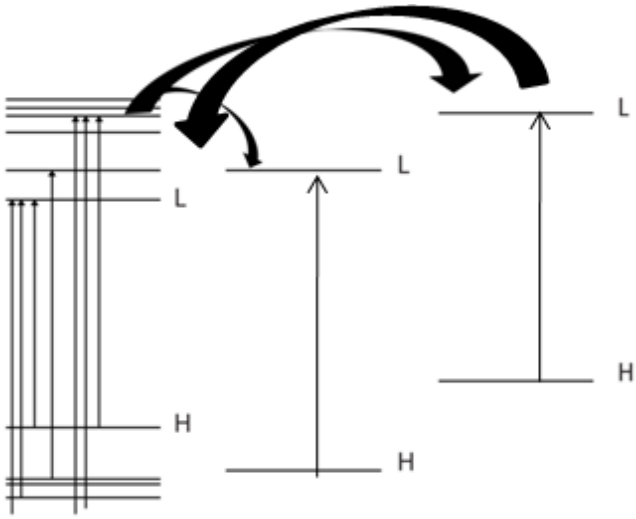


Seed 5 Seed 5 mena_keto mena_enol

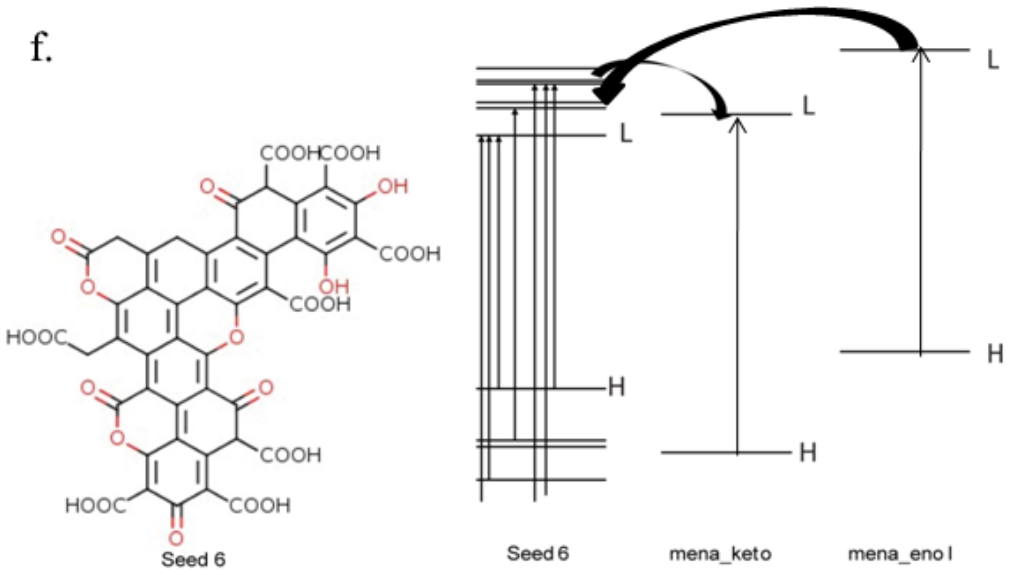


**Figure S14:** Probable electron transfer from **LUMO** of **pCD-DTTs**' surface tethered Seeds 1-6 (a→f) to menadione (keto & enol form).

(1) Sengupta, C.; Sarangi, M. K.; Sau, A.; Mandal, D.; Basu, S. A case study of photo induced electron transfer between riboflavin and aliphatic amine: Deciphering different mechanisms of ET operating from femtosecond to microsecond time domain. *Journal of Photochemistry and Photobiology A: Chemistry* **2015**, *296*, 25-34.

(2) Hanwell, M. D.; Curtis, D. E.; Lonie, D. C.; Vandermeersch, T.; Zurek, E.; Hutchison, G. R. Avogadro: an advanced semantic chemical editor, visualization, and analysis platform. *Journal of cheminformatics* **2012**, *4*, 17.

(3) Martínez, L.; Andrade, R.; Birgin, E. G.; Martínez, J. M. PACKMOL: a package for building initial configurations for molecular dynamics simulations. *Journal of computational chemistry* **2009**, *30*, 2157-2164.

(4) Bowers, K. J.; Chow, E.; Xu, H.; Dror, R. O.; Eastwood, M. P.; Gregersen, B. A.; Klepeis, J. L.; Kolossvary, I.; Moraes, M. A.; Sacerdoti, F. D. In *Tilte*2006; ACM.

(5) Harder, E.; Damm, W.; Maple, J.; Wu, C.; Reboul, M.; Xiang, J. Y.; Wang, L.; Lupyan, D.; Dahlgren, M. K.; Knight, J. L. OPLS3: a force field providing broad coverage of drug-like small molecules and proteins. *Journal of chemical theory and computation* **2015**, *12*, 281-296.

(6) Humphrey, W.; Dalke, A.; Schulten, K. VMD: visual molecular dynamics. *Journal of molecular graphics* **1996**, *14*, 33-38.

(7) Bera, K.; Sau, A.; Mondal, P.; Mukherjee, R.; Mookherjee, D.; Metya, A.; K. Kundu, A.; Mandal, D.; Satpati, B.; Chakrabarti, O.; Basu, S. Metamorphosis of Ruthenium-Doped Carbon Dots: In Search of the Origin of Photoluminescence and Beyond. *Chemistry of Materials* **2016**, *28*, 7404-7413.